

Generative Semantic Communication for Joint Image Transmission and Segmentation

Weiwen Yuan^{*†§}, Jinke Ren^{*†§}, Chongjie Wang^{*†§}, Ruichen Zhang[‡], Jun Wei[¶], Dong In Kim[◇], Shuguang Cui^{†*§}

^{*}FNii-Shenzhen, [†]SSE, and [§]Guangdong Provincial Key Laboratory of Future Networks of Intelligence,

The Chinese University of Hong Kong (Shenzhen), Shenzhen, China

[‡]College of Computing and Data Science, Nanyang Technological University, Singapore

[¶]College of Computer Science and Software Engineering, Shenzhen University, Shenzhen, China

[◇]Department of Electrical and Computer Engineering, Sungkyunkwan University, Suwon, South Korea

E-mail: {223010145, 223010039}@link.cuhk.edu.cn; {jinkeren, shuguangcui}@cuhk.edu.cn;

ruichen.zhang@ntu.edu.sg; weijun@szu.edu.cn; dongin@skku.edu

Abstract—Semantic communication has emerged as a promising technology for enhancing communication efficiency. However, most existing research emphasizes single-task reconstruction, neglecting model adaptability and generalization across multi-task systems. In this paper, we propose a novel generative semantic communication system that supports both image reconstruction and segmentation tasks. Our approach builds upon semantic knowledge bases (KBs) at both the transmitter and receiver, with each semantic KB comprising a source KB and a task KB. The source KB at the transmitter leverages a hierarchical Swin-Transformer, a generative AI scheme, to extract multi-level features from the input image. Concurrently, the counterpart source KB at the receiver utilizes hierarchical residual blocks to generate task-specific knowledge. Furthermore, the two task KBs adopt a semantic similarity model to map different task requirements into pre-defined task instructions, thereby facilitating the feature selection of the source KBs. Additionally, we develop a unified residual block-based joint source and channel (JSCC) encoder and two task-specific JSCC decoders to achieve the two image tasks. In particular, a generative diffusion model is adopted to construct the JSCC decoder for the image reconstruction task. Experimental results demonstrate that our multi-task generative semantic communication system outperforms previous single-task communication systems in terms of peak signal-to-noise ratio and segmentation accuracy.

I. INTRODUCTION

With the proliferation of artificial intelligence (AI) and the Internet of Things (IoT), there is an increasing demand for communication networks to support a growing number of devices and complex algorithms while conserving bandwidth and storage resources. Traditional communication technologies struggle to meet this demand by transmitting the original data, resulting in high bandwidth consumption. To address this challenge, semantic communication has been proposed to convey the intended meaning rather than raw data [1]. By transmitting only the semantic information relevant to specific tasks, semantic communication can significantly reduce the communication overhead, thereby saving bandwidth and enhancing transmission efficiency.

Recently, there have been many studies on semantic communication, which can be categorized into two classes. The

first one focuses on utilizing deep neural networks (DNNs) to extract semantic information for transmission [2]–[4], while the other emphasizes the establishment of semantic knowledge bases (KBs) to facilitate semantic coding and transmission [5]–[7]. For example, a hierarchical deep learning-based joint source-channel coding (JSCC) scheme was proposed in [3] to achieve the successive refinement of image transmission. Additionally, the authors of [4] introduced a deep learning-based JSCC scheme that incorporates channel output symbols into the transmission system to enhance the communication efficiency. Moreover, a semantic communication system based on a shared semantic KB was developed in [5], which combined the semantic information with the relevant knowledge from the semantic KB to reduce the communication overhead.

Although existing studies have achieved great success, they often focus on specific application scenarios with a single source modality, task objective, and communication environment. Therefore, the generalization and interpretability of these specific designs are often limited [8]. Some pioneering works have explored multi-task semantic communication [9], [10]. Specifically, the authors in [9] developed a Transformer-based framework for multi-user semantic communication, focusing on multimodal tasks like image retrieval, machine translation, and visual question answering. The authors in [10] presented a deep learning framework for multi-task image compression, using a coarse-to-fine structure and multi-attention networks to improve reconstruction quality. However, these approaches typically require storing multiple AI models at the transmitter and receiver to handle different tasks, presenting significant challenges for devices with limited storage resources. Moreover, when task requirements change, the models must be retrained, necessitating substantial communication and computational overhead.

To solve this problem, generative models offer a promising solution due to their powerful self-learning and generalization capabilities [11]–[13]. Our previous work [11] has introduced a new generative semantic communication architecture that used generative models to develop semantic KBs and facilitate semantic coding. Building on this, this paper considers developing a new multi-task generative semantic communication

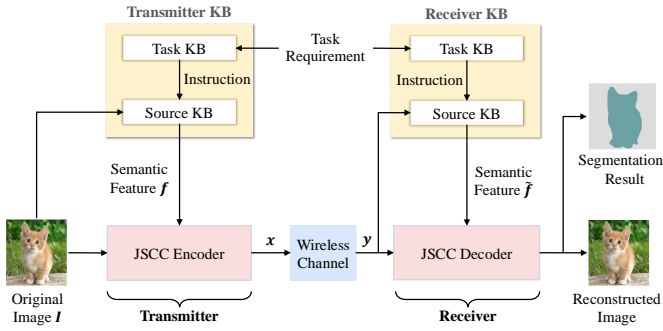


Fig. 1: Generative semantic communication system for joint image reconstruction and segmentation.

system by deploying semantic KBs at both the transmitter and receiver. In particular, each semantic KB comprises two components: a source KB and a task KB. The source KB at the transmitter employs a new generative model called Swin-Transformer [14] to extract multi-level semantic features from the source data, while the source KB at the receiver uses a ResNet model [15] to generate task-specific knowledge for JSCC decoding. The task KB guides the source KB to select approximate features according to the task requirement. Specifically, as task complexity increases, higher-level semantic features should be transmitted. For instance, in image reconstruction, the transmitter needs to extract both shallow and deep features, while in image segmentation, only shallow features are necessary. We evaluate the proposed system on two tasks of image reconstruction and image segmentation. The experimental results show that our proposed system outperforms traditional communication systems and classical semantic communication systems.

The rest of this paper is structured as follows. Section II introduces the generative semantic communication system model. Section III and Section IV present the detailed design of the semantic KBs and the JSCC coding module, respectively. Section V provides the simulation results and Section VI concludes the paper.

II. MULTI-TASK GENERATIVE SEMANTIC COMMUNICATION SYSTEM

A. System Model

As shown in Fig. 1, we consider a point-to-point semantic communication system, where a transmitter has an input image and a receiver aims to achieve the tasks of image reconstruction and segmentation. To facilitate semantic coding, two semantic KBs are deployed at both the transmitter and receiver. Each semantic KB is composed of a source KB and a task KB. The detailed working mechanism is as follows:

- The task requirement is input into the task KBs at both transmitter and receiver, which align the task requirement with a predefined task list and provide the corresponding task instructions to the source KBs.

- The original image I is input into the source KB at the transmitter, which outputs the key semantic feature f to the JSCC encoder.
- The JSCC encoder obtains the transmitted signal x by jointly processing the semantic feature f and the original image I .
- The transmitter sends the signal x to the receiver through a wireless channel, where the received signal can be expressed as

$$y = hx + n, \quad (1)$$

where h denotes the channel coefficient, $n \sim \mathcal{CN}(0, \sigma^2 U)$ represents an independent and identically distributed circularly symmetric complex Gaussian noise vector with an average noise power of σ^2 , and U is an identity matrix.

- The received signal y is input into the receiver's KB and the JSCC decoder, where the source KB at the receiver generates a task-specific image feature vector \tilde{f} according to the instructions provided by task KB.
- The feature vector \tilde{f} is input into the JSCC decoder, which integrates it with the received signal y to generate the desired results.

B. Task Description

To evaluate the proposed system, we consider two tasks of image reconstruction and image segmentation.

Image Reconstruction. In this task, the receiver aims to reconstruct the original images. The quality of the reconstructed images is evaluated by the peak signal-to-noise ratio (PSNR), which quantifies the ratio between the maximum possible pixel value and the power of the noise and is defined as

$$\text{PSNR} = 10 \log_{10} \left(\frac{\text{MAX}^2}{\text{MSE}} \right), \quad (2)$$

where MAX is the maximum possible pixel value in the image and MSE denotes the mean squared error between the original image I and the reconstructed image \hat{I} . A larger PSNR value indicates a better reconstructed image.

Image Segmentation. In this task, the receiver aims to divide an image into distinct regions, enabling a detailed analysis and understanding of its contents. Each pixel in the image is assigned a label, differentiating between various semantic categories. To optimize the segmentation process, the cross-entropy loss is calculated for each pixel. Moreover, the performance of image segmentation is typically assessed using intersection over union (IoU), which is defined as

$$\text{IoU} = \frac{|A \cap B|}{|A \cup B|}, \quad (3)$$

where A represents the predicted segmentation result and B is the ground-truth result. The numerator $|A \cap B|$ and denominator $|A \cup B|$ denote the overlap and union between A and B , respectively. The IoU ranges from 0 (no overlap) to 1 (complete overlap), directly measuring the percentage of correctly classified pixels.

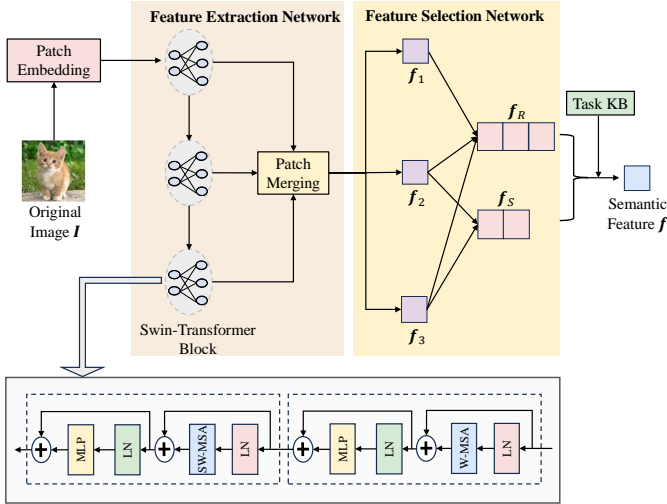


Fig. 2: An illustration of the KB at the transmitter.

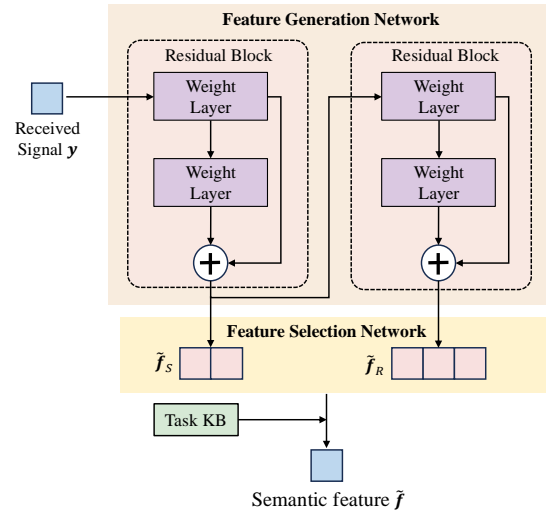


Fig. 3: An illustration of the KB at the receiver.

III. CONSTRUCTION OF SEMANTIC KBS

In this section, we present the detailed design of the semantic KBS. We first introduce the two task KBS and then present the source KBS at the transmitter and receiver, respectively.

A. Task KB

In this work, we establish two identical task KBS at the transmitter and receiver, which aim to map the complex task requirement in natural language into a predefined task instruction in the form of discrete tokens. The task KB consists of a memory module and a computing module. The memory module stores predefined task instructions, i.e., image reconstruction and image segmentation. The computing module is used to calculate the semantic similarity score. Specifically, upon receiving a task requirement, the computing module converts it into vector representations and computes the semantic similarity score between the vectors and each task instruction using the Sentence-BERT model [16]. The semantic similarity score is defined as

$$\text{Sim}(r, t_i) = \cos \left(\frac{\mathbf{v}(r) \cdot \mathbf{v}(t_i)}{\|\mathbf{v}(r)\| \|\mathbf{v}(t_i)\|} \right), \quad (4)$$

where r denotes the task requirement, t_i represents the i -th task instruction, and $\mathbf{v}(r)$ and $\mathbf{v}(t_i)$ are their vector representations, respectively. Then, the task KB selects the task instruction with the highest semantic similarity score and delivers it to the source KB for further processing.

B. Source KB at the Transmitter

The structure of the source KB at the transmitter is shown in Fig. 2. It consists of a feature extraction network and a feature selection network.

The feature extraction network is based on a powerful generative model called Swin-Transformer, which is shown at the bottom of Fig. 2. Specifically, the feature extraction

network employs a hierarchical architecture with three Swin-Transformers to generate hierarchical features, capturing semantic information at various levels. In particular, the feature extracted by the first Swin-Transformer captures the low-level information (i.e., edges and textures). In contrast, the features extracted by the second and third Swin-Transformer capture mid-level information (i.e., local shapes and patterns) and high-level information (i.e., object categories and complex patterns), respectively. The extracted hierarchical features are then processed through patch merging, which compresses spatial information while enhancing feature representation, thereby enabling more efficient downstream processing.

Let $\mathbf{f}_1, \mathbf{f}_2, \mathbf{f}_3$ denote the low-level, mid-level, and high-level features after patch merging, respectively. These features are then passed through the feature selection network, which selects task-relevant features based on the task instruction provided by the task KB. Specifically, since the image reconstruction task requires fine details like edges and colors, we aggregate all features of $\mathbf{f}_1, \mathbf{f}_2$, and \mathbf{f}_3 to improve reconstruction quality. The aggregated feature is denoted by $\mathbf{f}_R = \mathbf{f}_1 + \mathbf{f}_2 + \mathbf{f}_3$. In contrast, the image segmentation task is not sensitive to low-level features. Therefore, we only utilize \mathbf{f}_2 and \mathbf{f}_3 to reduce communication overhead. The aggregated feature is computed by $\mathbf{f}_S = \mathbf{f}_2 + \mathbf{f}_3$.

C. Source KB at the Receiver

As shown in Fig. 3, the source KB at the receiver also consists of two components, i.e., a feature generation network and a feature selection network.

The feature generation network employs two residual blocks that leverage residual connections for efficient feature learning. This architecture progressively generates deep features from the received signal through sequential convolution operations. In each residual block, the noisy signal \mathbf{y} is processed through two convolutional neural network (CNN) layers, transforming it into a deeper feature. The residual connection provides a

direct path for input features, mitigating the vanishing gradient problem during training. Moreover, the residual connection can simplify the learning of feature mappings for each layer, thereby resulting in a more compact feature representation.

The feature selection network is designed to identify task-relevant features from the outputs of the feature generation network. Specifically, since the image reconstruction task necessitates capturing fine details such as edges and colors, we combine all received features to restore rich image details. Conversely, for the image segmentation task that prioritizes global features, only high-level feature from the first residual block, i.e., \tilde{f}_S is utilized. By doing so, the segmentation performance can be guaranteed while the computational overhead is also reduced.

IV. JOINT SOURCE-CHANNEL ENCODER AND DECODER

In this section, we present the designs of the JSCC encoder and decoder to achieve efficient image reconstruction and segmentation.

A. JSCC Encoder

To reduce communication overhead and computational complexity, we design a unified JSCC encoder for both image reconstruction and segmentation. The JSCC encoder is built upon a ResNet architecture [15], which incorporates downsampling layers to reduce spatial resolution. As shown in Fig. 1, the input of the JSCC encoder includes two parts, i.e., the original image I and the output feature f from the source KB at the transmitter. The JSCC encoder first concatenates the original image I and the output feature f . Then, the concatenated vector is processed by a residual block. To further decrease spatial dimensions and computational complexity, we incorporate downsampling in the JSCC encoder using a specified stride, facilitating multi-scale feature extraction. The final output of the JSCC encoder is the signal x , which is sent to the receiver for image reconstruction or segmentation.

B. JSCC Decoder

To meet specific task requirements, we design two independent JSCC decoders at the receiver. As shown in Fig. 1, the input of each JSCC decoder includes two parts, i.e., the received signal y and the semantic feature \tilde{f} output by the source KB at the receiver. In the following, we introduce the detailed designs of the two JSCC decoders.

JSCC Decoder for Image Reconstruction. For image reconstruction, we utilize a generative diffusion model to construct the JSCC decoder due to its powerful self-learning and generation capabilities [17]. Specifically, the inputs, i.e., \tilde{f} and y are partitioned into a series of patches, which undergo iterative processing with added time step embeddings to capture temporal context. Moreover, positional encoding is applied to each patch embedding to get spatial information. By doing so, both temporal and spatial information are retained throughout the image reconstruction process. These output embeddings are further refined through a multi-head attention mechanism, which captures the dependencies across different

embeddings, enhancing feature representation by focusing on relevant spatial and contextual relationships. After several iterations of attention-based refinement, the results are concatenated to reconstruct the image. In addition, an upsampling layer is employed to restore the image to its original resolution, followed by a residual block to improve the image quality.

In the training process, we adopt the MSE between the original image and the reconstructed image as the loss function for image reconstruction, which is expressed as

$$L_R = \frac{1}{N} \sum_{i=1}^N (p_i - \hat{p}_i)^2, \quad (5)$$

where N is the total number of pixels, p_i and \hat{p}_i represent the value of the i -th pixel in the original and reconstructed images, respectively.

JSCC Decoder for Image Segmentation. For image segmentation, we utilize a ResNet with two residual blocks to build the JSCC decoder. Each residual block processes the semantic feature \tilde{f} through convolution operations, with outputs from each block being added to the original input. This skip connection preserves essential spatial information across layers. Moreover, an upsampling operation is applied to restore the original resolution. Finally, a 1×1 convolution maps the upsampled features to class logits, obtaining the final segmented result.

In the training process, we calculate the cross entropy as the loss function for image segmentation, which is defined as

$$L_S = -\frac{1}{N} \sum_{i=1}^N \log \left(\frac{e^{m_{t_i, q_i}}}{\sum_{j=1}^C e^{m_{j, q_i}}} \right), \quad (6)$$

where t_i and q_i are the ground-truth and predicted classes of pixel i , m_{t_i, q_i} is the probability of the predicted class t_i equals the ground-truth class q_i , and C is the number of classes.

V. EXPERIMENTAL RESULT

In this section, we conduct experiments to demonstrate the effectiveness of the proposed method. All experiment codes are implemented in a Linux environment equipped with two NVIDIA Tesla A100 40GB GPUs.

A. Experimental Setup

Datasets. For the image reconstruction task, we use the DIV2K dataset [18] for training and utilize both low-resolution (224×224) and high-resolution (768×512) images for validation. For the image segmentation task, we use the PASCAL VOC dataset [19] for both training and validation.

Baselines. For the image reconstruction task, we consider four baseline methods: 1) JPEG+LDPC+QAM(16/64), which adopts conventional separate source and channel coding and utilizes classical QAM for modulation; 2) wireless image transmission transformer (WITT) [20], which uses Swin-Transformer to extract semantic information; 3) Deep JSCC [21], in which the JSCC encoder consists of five convolutional layers while the JSCC decoder uses transposed convolution layers to upsample the compressed feature maps back to

TABLE I: System Parameters

Module	Configuration	Value
Transmitter KB	Window size	7
	Patch size	4
	Attention head	3
	Embedding dim	96
Receiver KB	Conv2D layers	3
	Conv2D kernel size	3
JSCC encoder	Conv2D layers	3
	Conv2D kernel size	3
	Hidden dimension	128
JSCC decoder (reconstruction)	Depth	28
	Patch size	2
	Attention head	16
JSCC decoder (segmentation)	Conv2D layers	1
	Conv2D kernel size	3
	Drop out	0.1
	Num classes	21

the images; 4) ADJSCC [22], which dynamically adjusts the coding strategy to optimize resource utilization, achieving efficient transmission.

For the image segmentation task, we adopt two baseline methods: 1) JPEG+LDPC+QAM(16/64)+FCN, which uses conventional separate source and channel coding, while utilizing a fully-connected network [23] to segment images at the receiver; 2) Deeplab JSCC [24], which adopts the Deeplab network as the fundamental architectures for the JSCC encoder and decoder. Through atrous convolution, it effectively captures the multi-scale contextual information to complete the image segmentation task.

Model parameters. We conduct end-to-end training for all methods. In particular, we use AdamW as an optimizer, and the learning rate is set as 0.0001. The momentum coefficients are set as 0.5 and 0.999 with a weight decay of 0.01 to prevent overfitting. Other model parameters are listed in Table I.

B. Performance on Image Reconstruction

Fig. 4 and Fig. 5 show the performance comparison of the proposed framework with the other four baselines for both low-resolution and high-resolution images. In the low-resolution image case, our method consistently achieves the best reconstruction performance among all methods, particularly outperforming the ADJSCC and WITT. This result highlights the importance of semantic KBs in image reconstruction. In the high-resolution image case, our method performs slightly better than that of other baselines when SNR is low. This is because high-resolution images contain more texture information than low-resolution images. As a result, even minor noise or pixel loss will significantly affect the perceived quality of the reconstructed image. Therefore, the impact of noise is more pronounced on high-resolution images when SNR is low. However, the performance gaps between our method and other baselines increase with SNR, which demonstrates the effectiveness of the proposed method when the communication environment is fine. For better comparison,

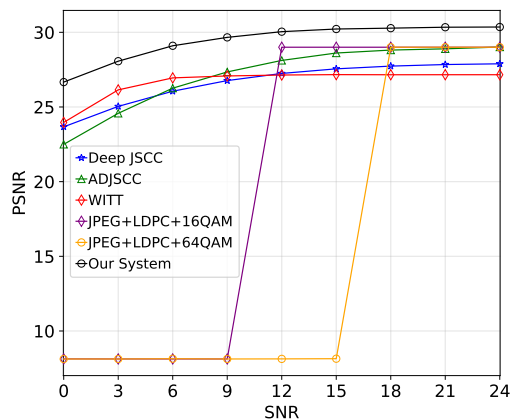


Fig. 4: PSNR v.s. SNR in low-resolution image case.

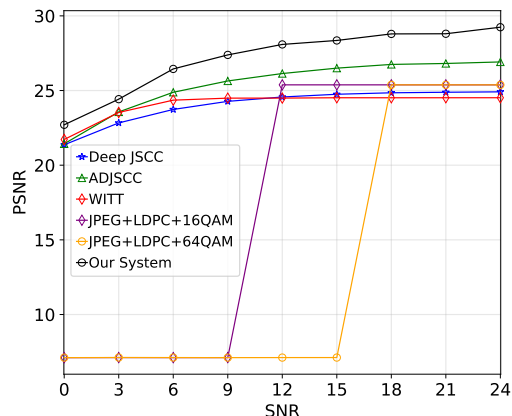


Fig. 5: PSNR v.s. SNR in high-resolution image case.

we visualize the reconstructed images of different methods when SNR = 18 dB, as shown in Fig. 6. It is observed that our method achieves the best visual quality with smooth facial details. More importantly, our framework achieves the lowest communication overhead among all methods.

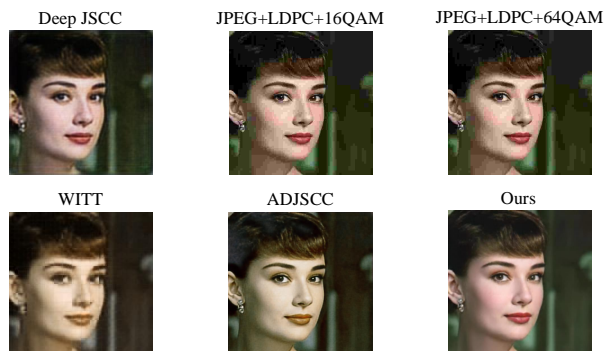


Fig. 6: Visualization of reconstructed images (SNR = 18dB).

C. Performance on Image Segmentation

Fig. 7 shows the image segmentation performance of all methods. For a fair comparison, the communication overhead

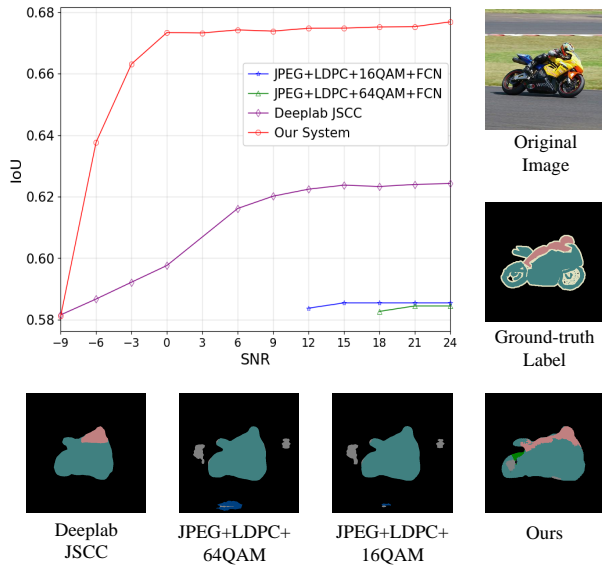


Fig. 7: Segmentation accuracy and visualization results of different methods.

of all methods is bounded by 20 Kbits. It is seen that under the same communication overhead, our method achieves the highest image segmentation accuracy compared to other baseline methods. In particular, when the SNR is greater than 0dB, the performance of our method will stabilize, demonstrating its robustness. Moreover, for the LDPC+JPEG+QAM methods, when the SNR is low (<12 dB for 16QAM or <18 dB for 64QAM), the receiver cannot accurately reconstruct the original image. Therefore, the FCN model cannot perform effective image segmentation, such that the image segmentation accuracy under low SNR is omitted. The bottom half of Fig. 7 provides the visualization results of all methods. It is seen that the segmentation result of our method is consistent with the ground-truth label, which not only identifies the target objects but also preserves the edge details. In contrast, the Deeplab JSCC cannot accurately distinguish the target object, while the boundaries are blurred. The traditional LDPC+JPEG+QAM methods perform even worse with erroneous areas in the segmentation results.

VI. CONCLUSION

In this paper, we propose a generative semantic communication system for both image transmission and segmentation. Two generative AI schemes of Swin-Transformer and diffusion model are adopted to build the semantic KBs and JSCC decoder, significantly reducing the data traffic while improving the communication efficiency. Numerical results show that our method can achieve better performance than several baseline methods. Our designs reveal the potential of using generative AI schemes for simultaneously handling multiple tasks and provide a new direction for achieving multi-task generative semantic communication.

REFERENCES

- [1] W. Weaver, "Recent contributions to the mathematical theory of communication," *ETC: a review of general semantics*, pp. 261–281, 1953.
- [2] H. Xie, Z. Qin, G. Y. Li, and B.-H. Juang, "Deep learning enabled semantic communication systems," *IEEE Trans. Signal Process.*, vol. 69, pp. 2663–2675, Apr. 2021.
- [3] D. B. Kurka and D. Gündüz, "Successive refinement of images with deep joint source-channel coding," in *Proc. IEEE Int. Workshop Signal Process. Adv. Wireless Commun.*, Cannes, France, Jul. 2019, pp. 1–5.
- [4] D. B. Kurka and D. Gündüz, "DeepJSCC-f: Deep joint source-channel coding of images with feedback," *IEEE J. Sel. Areas Inf. Theory*, vol. 1, no. 1, pp. 178–193, May. 2020.
- [5] P. Yi, Y. Cao, X. Kang, and Y.-C. Liang, "Deep learning-empowered semantic communication systems with a shared knowledge base," *IEEE Trans. Wireless Commun.*, vol. 23, no. 6, pp. 6174–6187, Jun. 2023.
- [6] X. Xu, H. Xiong, Y. Wang, Y. Che, S. Han, B. Wang, and P. Zhang, "Knowledge-enhanced semantic communication system with OFDM transmissions," *Sci. China Inf. Sci.*, vol. 66, no. 7, p. 172302, 2023.
- [7] J. Zheng, J. Ren, P. Xu, Z. Yuan, J. Xu, F. Wang, G. Gui, and S. Cui, "Generative semantic communication for text-to-speech synthesis," *arXiv preprint arXiv:2410.03459*, 2024.
- [8] S. Jiang, Y. Liu, Y. Zhang, P. Luo, K. Cao, J. Xiong, H. Zhao, and J. Wei, "Reliable semantic communication system enabled by knowledge graph," *Entropy*, vol. 24, no. 6, p. 846, Apr. 2022.
- [9] H. Xie, Z. Qin, X. Tao, and K. B. Letaief, "Task-oriented multi-user semantic communications," *IEEE J. Sel. Areas Commun.*, vol. 40, no. 9, pp. 2584–2597, Jul. 2022.
- [10] Z. Zhang, Q. Yang, S. He, and Z. Shi, "Semantic communication approach for multi-task image transmission," in *Proc. IEEE Veh. Technol. Conf. (VTC-Fall)*, London, United Kingdom, Sep. 2022, pp. 1–2.
- [11] J. Ren, Z. Zhang, J. Xu, G. Chen, Y. Sun, P. Zhang, and S. Cui, "Knowledge base enabled semantic communication: A generative perspective," *IEEE Wireless Commun.*, vol. 31, no. 4, pp. 14–22, 2024.
- [12] R. Zhang *et al.*, "Generative ai agents with large language model for satellite networks via a mixture of experts transmission," *IEEE J. Sel. Areas Commun (early access)*, 2024.
- [13] R. Zhang, H. Du, Y. Liu, D. Niyato, J. Kang, S. Sun, X. Shen, and H. V. Poor, "Interactive ai with retrieval-augmented generation for next generation networking," *IEEE Network (early access)*, 2024.
- [14] Z. Liu *et al.*, "Swin transformer: Hierarchical vision transformer using shifted windows," in *Proc. IEEE Conf. Comput. Vis. Pattern Recognit. (CVPR)*, Virtual, Oct. 2021, pp. 10012–10022.
- [15] S. Targ, D. Almeida, and K. Lyman, "Resnet in resnet: Generalizing residual architectures," *arXiv preprint arXiv:1603.08029*, Mar. 2016.
- [16] N. Reimers, "Sentence-bert: Sentence embeddings using siamese bert-networks," *arXiv preprint arXiv:1908.10084*, Aug. 2019.
- [17] W. Peebles and S. Xie, "Scalable diffusion models with transformers," in *Proc. IEEE Conf. Comput. Vis. Pattern Recognit. (CVPR)*, Paris, France., Oct. 2023, pp. 4195–4205.
- [18] E. Agustsson and R. Timofte, "Ntire 2017 challenge on single image super-resolution: Dataset and study," in *Proc. IEEE Conf. Comput. Vis. Pattern Recognit. Workshops*, Honolulu, USA, Aug. 2017, pp. 126–135.
- [19] M. Everingham, L. Van Gool, C. K. Williams, J. Winn, and A. Zisserman, "The pascal visual object classes (voc) challenge," *Int. J. Comput. Vis.*, vol. 88, pp. 303–338, Sep. 2009.
- [20] K. Yang, S. Wang, J. Dai, K. Tan, K. Niu, and P. Zhang, "Witt: A wireless image transmission transformer for semantic communications," in *Proc. IEEE Int. Conf. Acoust. Speech Signal Process. (ICASSP)*, Rhodes Island, Greece, May. 2023, pp. 1–5.
- [21] E. Bourtsoulatzé, D. B. Kurka, and D. Gündüz, "Deep joint source-channel coding for wireless image transmission," *IEEE Trans. Cognit. Commun. Networking*, vol. 5, no. 3, pp. 567–579, Sep. 2019.
- [22] J. Xu, B. Ai, W. Chen, A. Yang, P. Sun, and M. Rodrigues, "Wireless image transmission using deep source channel coding with attention modules," *IEEE Trans. Circ. Syst. Video Tech.*, vol. 32, no. 4, pp. 2315–2328, May. 2021.
- [23] K. He, X. Zhang, S. Ren, and J. Sun, "Deep residual learning for image recognition," in *Proc. IEEE Conf. Comput. Vis. Pattern Recognit. (CVPR)*, Las Vegas, Nevada., Jun. 2016, pp. 770–778.
- [24] L.-C. Chen, G. Papandreou, I. Kokkinos, K. Murphy, and A. L. Yuille, "Deeplab: Semantic image segmentation with deep convolutional nets, atrous convolution, and fully connected crfs," *IEEE Trans. Pattern Anal. Mach. Intell.*, vol. 40, no. 4, pp. 834–848, Apr. 2017.